Pericyte Loss and Microaneurysm Formation in PDGF-B–Deficient Mice

Per Lindahl, Bengt R. Johansson, Per Levéen,* Christer Betsholtz†

Platelet-derived growth factor (PDGF)–B–deficient mouse embryos were found to lack microvascular pericytes, which normally form part of the capillary wall, and they developed numerous capillary microaneurysms that ruptured at late gestation. Endothelial cells of the sprouting capillaries in the mutant mice appeared to be unable to attract PDGF-Rβ–positive pericyte progenitor cells. Pericytes may contribute to the mechanical stability of the capillary wall. Comparisons made between PDGF null mouse phenotypes suggest a general role for PDGFs in the development of myofibroblasts.

Platelet-derived growth factor–B, a high-affinity ligand for the receptor tyrosine kinases PDGF-Rα and -β, promotes proliferation and migration of mesenchymal cells in vitro (*1–3*). Disruption of the PDGF-B or PDGF-Rβ genes in mice leads to the development of lethal hemorrhage and edema in late embryogenesis and absence of kidney glomerular mesangial cells (*4, 5*). Mesangial cells are related to microvascular pericytes (*6*), which are contractile cells similar to smooth muscle cells that encircle microvessels in many different tissues (*7*). Pericytes express PDGF receptors and respond to PDGF in vitro (*8, 9*). We here identify deficient pericyte development as the underlying cause of hemorrhage in PDGF-B mutants.

Pericytes have been identified morphologically in the embryonic rat brain (*10*). We analyzed the effect of PDGF-B deficiency on pericyte formation in the developing mouse brain (*11*). We chose the latest time point, embryonic day (E) 16.5, at which most PDGF-B–deficient (PDGF-B −/−) embryos (*12*) remained alive and without signs of hemorrhaging. Capillaries in brains were scored for the presence or absence of pericytic cell bodies and cytoplasmic processes. The data from these analyses are presented in Table 1. Notably, 40/213 sectioned PDGF-B +/+ or +/− capillaries showed associated pericytes sectioned through the nucleus, whereas the corresponding number for PDGF-B −/− capillaries was 0/173. When capillaries with associated cytoplasmic processes (pericytic or endothelial) were included, the numbers were 175/213 for PDGF-B +/+ or +/− and 7/173 for PDGF-B −/− capillaries. Naked endothelial tubes were scored in 13/213 cases in PDGF-B +/+ or +/−, and in 153/173 cases in PDGF-B −/− capillaries. Representative examples from the electron microscopy (EM) studies are shown in Fig. 1.

Through gestational days E12.5 to E16.5, PDGF-B was expressed in the endothelium of many capillaries and small arteries and in liver megakaryocytes at E14.5 and later (*13*) [Fig. 2A and (*14*)]. There was no detectable expression of PDGF-B in venous endothelium, in the endocardium, or in aortic endothelium (*14*). PDGF-Rβ mRNA was expressed in developing vascular walls. Larger arteries, but not veins, were surrounded by several layers of PDGF-Rβ–positive mesenchymal cells, smaller arteries by single layers, and capillaries by a non-continuous layer of PDGF-Rβ–positive cells (Figs. 2, B, C, E, G, and I, and 3, A to F). The location and distribution of the latter cells was typical of pericytes (Figs. 2B and 3, A to D). PDGF-Rβ–positive cells were also abundant in capillary plexa (for example, the perineural plexus, in developing endocrine organs, and in plexus choroideus) [Fig. 2, C and I) and (*14*)]. PDGF-Rα was expressed at various sites in the mesenchyme at E12.5–16.5, without specific association with developing blood vessels (*14*). These embryonic expression patterns of PDGF-B and PDGF-Rβ imply the existence of paracrine signaling, involving this li-

Table 1. Quantitation of pericyte elements in association with microvessels in E16.5 mouse brains. Microvessels with whole lumina that were encountered in EM sections were counted and classified into the following categories: (a) naked endothelial tubes; (b) pericyte processes present (figures might represent an overestimation because abluminal folds and overlappings of endothelial cells could be misinterpreted as pericyte processes); (c) microvessels with pericytes sectioned through the nucleus; (d) lumina are part of a clear sprout (because of the presence of a highly convoluted microvessel cell surface in sprouts, the classification into endothelial or pericytic elements is difficult and was avoided); and (e) not possible to classify in other categories, for example, because of oblique sectioning. The total number of PDGF-B −/− microvessels analyzed was 173. The total number of PDGF-B +/+ or +/− microvessels analyzed was 213.

Embryos (genotype)	Microvessel category				
	a	b	c	d	e
1 (−/−)	50	6	0	4	0
2 (−/−)	47	0	0	4	1
3 (−/−)	46	1	0	2	2
Sum	153	7	0	10	3
4 (+/+ or +/−)	2	42	11	5	0
5 (+/+ or +/−)	2	35	14	4	5
6 (+/+ or +/−)	4	21	6	2	0
7 (+/+ or +/−)	5	37	9	7	2
Sum	13	135	40	18	7

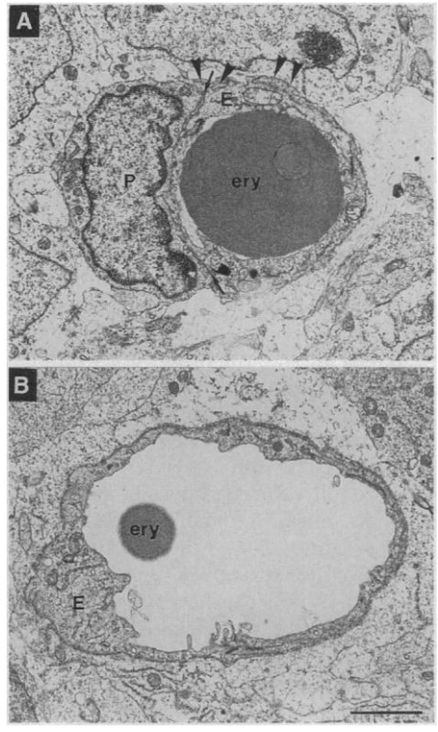

Fig. 1. Absence of brain pericytes in PDGF-B −/− mice. Electron micrograph mount of representative cross-sectioned capillaries that illustrate consistent differences in the deep brain cortex from (**A**) PDGF-B +/+ and (**B**) −/− E16.5 embryos. The P label in (A) is on the pericyte nucleus, which is surrounded by a thin rim of cytoplasm. The arrows in (A) point to the border between the pericyte cytoplasm and the endothelial cell (E label) cytoplasm. The arrowheads in (A) point to pericyte processes (pericytic cytoplasm embedded in the endothelial cell basement membrane). The endothelial cell nucleus is not visible. Note the dilation of the PDGF-B −/− capillary in (B) (typical in the mutant) compared with the PDGF-B +/+ capillary in (A). Ery, erythrocyte. Bar = 2.5 μm.

P. Lindahl, P. Levéen, C. Betsholtz, Department of Medical Biochemistry, University of Göteborg, Medicinaregatan 9A, S-413 90 Göteborg, Sweden.
B. R. Johansson, Department of Anatomy and Cell Biology, University of Göteborg, Medicinaregatan 9A, S-413 90 Göteborg, Sweden.
*Present address: Wallenberg Neurocenter, University of Lund, Sölve-gantan 17, S-223 62 Lund, Sweden.
†To whom correspondence should be addressed. E-mail: christer.betsholtz@medkem.gu.se

gand-receptor pair, from vascular endothelium to vascular wall progenitors.

PDGF-Rβ expression was altered in some but not all tissues of PDGF-B −/− embryos. At E14.5–17.5, PDGF-Rβ–positive pericytes normally found in wild-type embryos were absent from PDGF-B −/− brain, heart, lung, and brown adipose tissue (Fig. 2, C to F) (*14*). The PDGF-Rβ expression at other sites (in arterial walls and in vascular plexa) seemed unaffected. In wild-type E12.5 embryos, PDGF-Rβ was mainly expressed in developing arterial walls, but a few scattered PDGF-Rβ–positive cells were also associated with neighboring microvessels and appeared to have migrated to these sites from the arterial wall location (Fig. 2G). In PDGF-B −/− E12.5 embryos, PDGF-Rβ was expressed in arterial walls, but no scattered PDGF-Rβ–positive cells were found surrounding microvessels (Fig. 2H). Similarly, PDGF-Rβ–positive cells, which normally migrate into the brain together with capillaries growing in from the perineural vascular plexus (Fig. 2I), were absent from E12.5

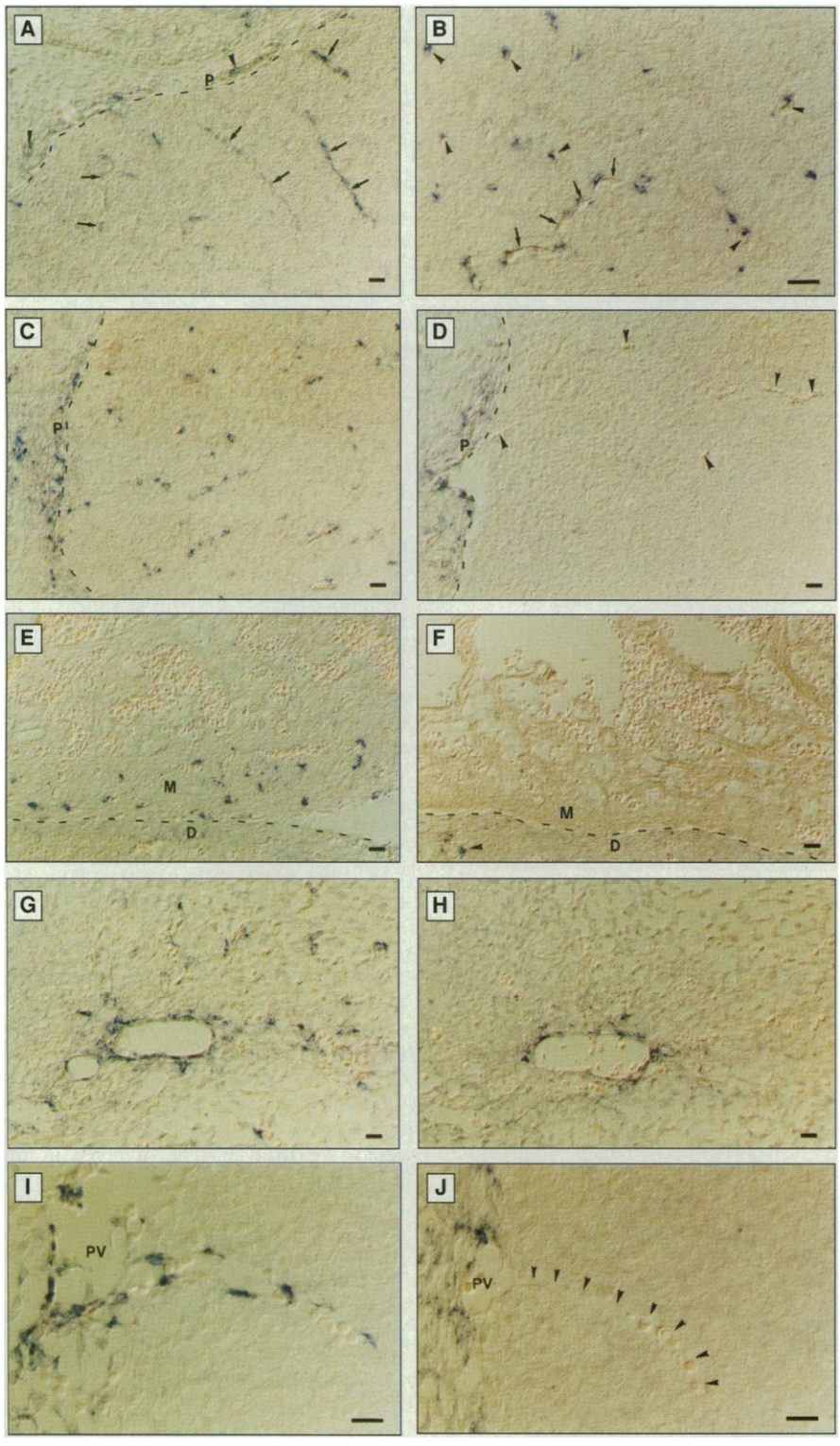

Fig. 2. PDGF-B and PDGF-Rβ expression patterns. Nonradioactive in situ hybridization of PDGF-B +/+ (A, B, C, E, G, and I) and PDGF-B −/− (D, F, H, and J) sections. (**A**) PDGF-B expression in the brain and perineural plexus of an E14.5 embryo. PDGF-B is expressed in capillaries (arrows) and in larger blood vessels of the perineural plexus (arrowheads). P, perineural plexus. (**B**) PDGF-Rβ expression in the E14.5 brain. A longitudinally sectioned erythrocyte-containing capillary is shown (arrows) as are several cross-sectioned capillaries (arrowheads). More than 95% of the PDGF-Rβ–positive cells were seen in close proximity to capillaries. Note the difference between the capillary endothelial staining for PDGF-B shown in (A) compared with the pericapillary, pericytic staining for PDGF-Rβ seen in (B). (**C** and **D**) A comparison between the PDGF-Rβ expression patterns in the brain of PDGF-B +/+ (C) and PDGF-B −/− (D) E14.5 embryos. Pericapillary staining for PDGF-Rβ is completely absent in the PDGF-B −/− brain, whereas PDGF-Rβ staining in the perineural plexus (P) is seen in both genotypes. The presence of capillaries is indicated in the PDGF-B −/− brain (arrowheads). (**E** and **F**) A comparison between the PDGF-Rβ expression patterns in the heart of PDGF-B +/+ (E) and PDGF-B −/− (F) E14.5 embryos. Note the complete absence of pericapillary PDGF-Rβ staining in the PDGF-B −/− heart. PDGF-Rβ–positive cells surrounding a small artery in the diaphragm (D) are shown (arrowhead). The thin and hypertrabeculated myocardium (M) in the PDGF-B −/− section is a hallmark of the phenotype of these mice (*4*). (**G** to **J**) Spreading of PDGF-Rβ–positive cells in response to PDGF-B at E12.5. (G) and (H) show the internal carotid artery and surrounding mesenchyme in PDGF-B +/+ (G) and PDGF-B −/− (H) embryos. In the PDGF-B +/+ tissue, PDGF-Rβ–positive cells are situated in the developing arteric wall and as a scattered population of cells in close contact with surrounding microvessels. In the PDGF-B −/− tissue, the scattered population of PDGF-Rβ–positive cells is specifically lost, whereas arterial wall expression remains. (I) and (J) show the perineural plexus and a capillary extending from the plexus vasculature (PV) into the developing brain in a PDGF-B +/+ (I) and a PDGF-B −/− (J) E12.5 embryo. Note the presence of PDGF-Rβ–positive cells in the plexus of both embryos, but the specific absence of PDGF-Rβ–positive cells in contact with the ingrowing capillary in the PDGF-B −/− embryo (arrowheads). Bars = 40 μm.

PDGF-B −/− embryos (Fig. 2J).

Many tissues in PDGF-B −/− embryos at late gestation have dilated microvessels (*14*). To study the capillary morphology in more detail, we crossed mice carrying one copy of the PDGF-B null allele with mice carrying a lacZ reporter gene driven by the TIE1 promoter (tie^{lcz}) (*15*). From subsequent intercrosses tie^{lcz} heterozygous embryos being either PDGF-B +/+, +/−, or −/− were selected at time points before the onset of hemorrhaging. Horizontal or frontal brain sections (50 μm thick) were stained for lacZ expression (*16*) to highlight the architecture of capillaries (Fig. 4). Whereas PDGF-B +/+ or +/− capillaries were straight and had a uniform diameter (~5 μm), PDGF-B −/− capillaries were tortuous, variable in diameter, and had numerous microaneurysms from 25 to 100 μm in diameter. Cylindrical dilations that occured over longer stretches were also seen. Some of the dilations appeared to reflect focal distensions in the capillary wall. However, increased endothelial cellularity was evident at many dilated sites, by both light microscopy and transmission electron microscopy, suggesting that the microaneurysm formation included a component of endothelial cell proliferation.

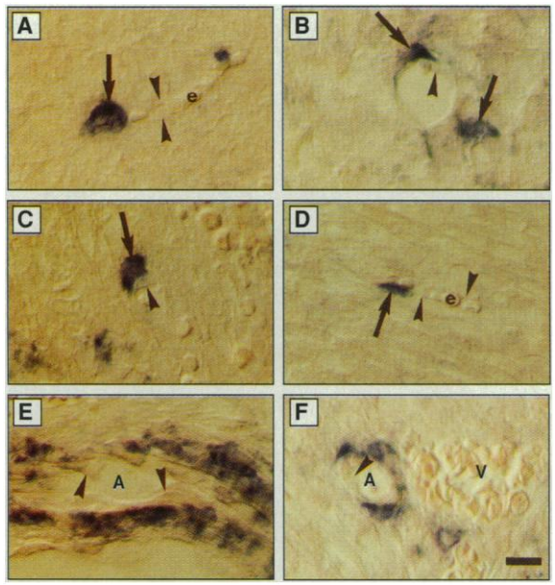

Fig. 3. High-magnification view of PDGF-Rβ expression at small blood vessels. Nonradioactive in situ hybridization was done on E14.5 PDGF-B +/+ embryos. (**A**) Brain microvessel; (**B**) skin microvessel; (**C**) capillary in myocardium; (**D**) capillary in skeletal muscle; (**E**) small artery in the lung; (**F**) intercostal artery and vein. Note that PDGF-Rβ–positive cells in (A) to (D) (arrows) have a pericytic location, that is, they are situated outside PDGF-Rβ–negative endothelial cells (arrowheads). In contrast to our conclusions on the pericytic expression of PDGF-Rβ, previous reports have suggested that developing capillary endothelial cells express PDGF-Rβ (*35*). This idea was based on radioactive in situ hybridization, which does not allow for the discrimination between capillary endothelial versus pericytic expression of PDGF-Rβ. A, artery; V, vein; e, erythrocyte; bar = 20 μm.

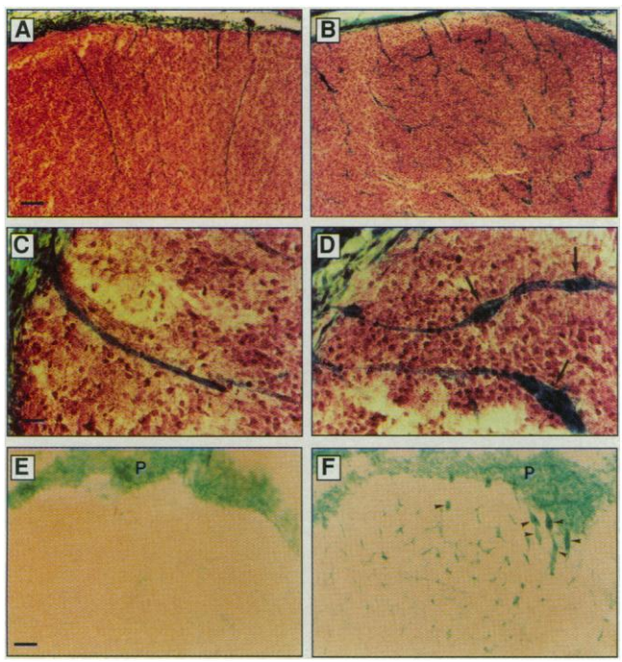

Fig. 4. Capillary morphology and expression of tie^{lcz} in PDGF +/+ (A, C, and E) and −/− (B, D, and F) embryos. (**A** and **B**) Brain stem sections (50 μm thick) from PDGF-B +/+ (A) and −/− (B) E18.5 embryos. tie^{lcz} staining occurs in blood vessels in the perineural plexus and in brain capillaries. Note the tortuous appearance of the capillaries in the PDGF-B −/− brain and the abundance of focal dilations (microaneurysms). Bar = 160 μm, and applies to (B). (**C** and **D**) Higher magnifications of brain stem capillaries. The capillaries in PDGF-B +/+ tissue were invariably straight and had a uniform diameter. In contrast, the PDGF-B −/− capillaries (D) showed the occurrence of numerous microaneurysms (arrows). Bar = 40 μm, and applies to (D). (**E** and **F**) Temporal lobe sections (50 μm thick) from E17.5 PDGF-B +/+ (E) and −/− (F) embryos. Up-regulated tie^{lcz} expression is seen in PDGF-B −/− capillaries with abnormal morphology in comparison with the normal capillaries in PDGF-B +/+ tissue. Some small-diameter capillaries in the PDGF-B −/− tissue also show low tie^{lcz} expression. The perineural plexus (P) staining is uniformly strong in both PDGF-B +/+ and −/− embryos. Note the abundance of microaneurysms in the PDGF-B −/− tissue (arrowheads). The development of the tie^{lcz} stain was for 24 hours in (A) to (D) and for 3 hours in (E) and (F). Bar = 160 μm, and applies to (F).

The tie^{lcz} stainings revealed up-regulated TIE1 expression in PDGF-B −/− brain capillary endothelium compared with that in PDGF-B +/+ and +/− embryos (Fig. 4). TIE1 up-regulation was also seen in capillaries in the PDGF-B −/− lung, heart, and adipose tissue, that is, at sites where pericyte loss was noticed (*14*). At other locations such as in small arterial endothelium and in capillary plexa, TIE1 expression was indistinguishable in PDGF-B −/−, +/−, and +/+ embryos [Fig. 4 and (*14*)].

Our data show that pericytes depend on PDGF-B for their development. PDGF-Rβ is expressed in developing pericytes. Without PDGF-B, pericytes fail to develop in capillaries formed through angiogenesis. Pericytes originate from progenitors in arterial walls and vascular plexa and migrate along capillary sprouts that express PDGF-B. Thus, PDGF-B stimulates PDGF-Rβ–positive vascular wall progenitors, which may result in both migration and proliferation. It is less likely that pericytes develop in situ by PDGF-B–mediated induction of progenitor cells because we found no detectable expression of PDGF-Rβ or -Rα in the brain of PDGF-B −/− embryos before E14.5. We would rather propose the existence of another endothelium-derived "inducing" factor or factors, the action of which leads to PDGF-Rβ up-regulation in mesenchymal cells surrounding arteries and plexus vasculature. Candidate mediators of such induction may include tissue factor (TF) because TF-deficient mouse embryos fail to develop vascular wall cells in vitelline blood vessels (*17*). Recent work also suggests that angiopoietin-1–TIE2 receptor signaling may be involved in the recruitment or differentiation (or both) of vascular smooth muscle cells (*18–23*). Because angiopoietin-1 is expressed by perivascular mesenchymal cells (*18*), and TIE2 by endothelial cells (*24*), their interaction may lead to endothelial release of the inducing factor or factors. Angiopoietin-1 or TIE2 null mice fail to develop smooth muscle cells surrounding large vessels and die at E9.5–12.5 (*19, 22, 23*). At this time PDGF-Rβ–positive vascular wall

cells form normally around arteries in PDGF-B −/− embryos (Fig. 2, G and H), and at E18.5 PDGF-B −/− embryos show a normal abundance of arterial smooth muscle cells (*4*).

The function of pericytes in vivo has been unclear, although their distribution has suggested they may support capillary structure (*7*). Pericytes may also regulate endothelial cell function. Studies of angiogenesis in vivo in response to wounding have suggested that pericyte appearance in the wound area correlates with inhibition of endothelial cell proliferation (*25*, *26*). Pericytes and smooth muscle cells also inhibit endothelial cell proliferation and migration in vitro (*27*, *28*). The development of abnormal capillaries in pericyte-deficient PDGF-B −/− embryos shows that pericytes regulate microvessel structure. In PDGF-B −/− embryos, microaneurysms, hemorrhages, and edema occur perinatally, when blood pressure increases. In addition, the spatial correlation between TIE1 up-regulation and pericyte loss seen in the PDGF-B −/− embryos, and the increased cellularity in many microaneurysms, imply that pericytes regulate gene expression and hence the differentiated functions of capillary endothelial cells. TIE1 is an endothelial cell receptor tyrosine kinase involved in blood vessel formation during embryogenesis (*15*, *23*) and possibly also in the adult (*29*). Its up-regulation may relate to the increased proliferation of endothelial cells in the microaneurysms.

The morphology of the microaneurysms formed in PDGF-B −/− embryos is similar to those in the retinal microvessels of diabetic individuals (*30*). Here also dilations were both spherical and cylindrical, frequently showed increased endothelial cellularity, and correlated with the loss of capillary mural cells (pericytes) (*30*, *31*). The pericyte-like kidney mesangial cells have been implicated in renal glomerulosclerosis, another aspect of diabetic vascular disease. The loss of mesangial cells in PDGF-B −/− and PDGF-Rβ −/− embryos (*4*, *5*) seems to occur by a mechanism similar to that of the pericyte loss: failure of recruitment of PDGF-Rβ–positive progenitors into the developing glumerular tuft (*32*). In glomerulosclerosis, increased deposition of extracellular matrix leads to a thickening of the glomerular basement membrane and increased deposition of mesangial matrix (*33*). In view of the similar ontogeny of pericytes and mesangial cells, it is intriguing that both appear to be involved in the pathogenesis of late complications in diabetes mellitus. Thus, common pathogenic mechanisms may underly pericyte and mesangial cell reaction in the pathogenesis of this disease.

Because pericytes (this study) and mesangial cells (*4*) are absent in PDGF-B −/− mice, and alveolar myofibroblasts are absent in PDGF-A −/− mice (*34*), PDGFs may be of general importance in the ontogeny of different types of myofibroblasts.

REFERENCES AND NOTES

1. C.-H. Heldin, *EMBO J.* **11**, 4251 (1992).
2. E. W. Raines, D. F. Bowen-Pope, R. Ross, in *Handbook of Experimental Pharmacology. Peptide Growth Factors and Their Receptors*, M. B. Sporn and A. B. Roberts, Eds. (Springer-Verlag, Heidelberg, 1990), pp. 173–262.
3. B. Westermark, C. e. Sorg, *Biology of Platelet-Derived Growth Factor* (Karger, Basel, 1993).
4. P. Levéen *et al.*, *Genes Dev.* **8**, 1875 (1994).
5. P. Soriano, *ibid.*, p. 1888.
6. D. Schlondorff, *FASEB J.* **1**, 272 (1987).
7. D. E. Sims, *Tissue Cell* **18**, 153 (1986).
8. L. R. Bernstein, H. Antoniades, B. R. Zetter, *J. Cell Sci.* **56**, 71 (1982).
9. P. A. D'Amore and S. R. Smith, *Growth Factors* **8**, 61 (1993).
10. K. Fujimoto, *Anat. Rec.* **242**, 562 (1995).
11. Embryo heads, divided by a coronal section at the level of the external auditory meatus, were immersed in 2.5% glutaraldehyde, 2% paraformaldehyde, and 0.02% sodium azide in 0.05 M Na cacodylate, pH 7.2, for 24 hours. About 1-mm-thick slices of fixed tissue were treated with 0.5% OsO_4 and 1% potassium ferrocyanate in 0.1 M Na cacodylate for 3 hours, followed by 1% tannic acid in water for 30 min. The tissue slices were dehydrated and flat embedded. Ultrathin sections encompassing cortical and subcortical regions were contrasted with uranyl acetate and lead citrate and examined in a Zeiss CEM 902 electron microscope.
12. PDGF-B +/− mice line 3.22 (*4*), bred as 129sv/C57B16 hybrids, were crossed, and embryos were derived by caesarean section at E16.5. Tail or yolk sac tissue was used for genotyping by a three-primer polymerase chain reaction (PCR). The forward primer 5′-GGGTGGGACTTTGGTGTAGAGAAG-3′ and the two reverse primers 5′-TTGAAGCGTGCAGAATGCC-3′ and 5′-GGAACGGATTTTGGAGGTAGTGTC-3′ yielded 265–base pair (bp) wild-type and 624-bp mutant allele products in a 40-cycle reaction (96°C for 30 s, 59.5°C for 30 s, 64°C for 2 min). *Tie*^{lcz} mice (*15*) represent heterozygous carriers of a lacZ coding sequence integrated in the TIE1 locus and, hence, under the transcriptional control of TIE1 regulatory elements. *Tie*^{lcz} mice were propagated by heterozygous breeding, and *Tie*^{lcz} carriers were identified by lacZ staining of tail tissue. *Tie*^{lcz} heterozygote mice were crossed with PDGF-B +/− mice to generate double heterozygote mice, which were subsequently crossed with PDGF-B +/− mice. From these crossings, *tie*^{lcz} heterozygote embryos being either PDGF-B −/− or PDGF-B +/+ were identified by PCR.
13. We used a modification of the protocol described in (*34*). Briefly, embryos were fixed overnight in 4% buffered paraformaldehyde (PFA), cryosectioned, and stored at −20°C. Before hybridization, sections were treated with proteinase K (10 μg/ml) and refixed in PFA for 15 min. Prehybridization occured in a solution containing 50 to 55% deionized formamide (55% was used for the PDGF-B probe and 50% for all other probes), 10% dextran sulphate, yeast tRNA (1 mg/ml), 1× Denhardt's solution, 5 mM EDTA, 0.2 M NaCl, 0.013 M tris-HCl, 5 mM NaH_2PO_4, and 5 mM $NaHPO_4$, pH 7.5. Heated probes (see below) were added at a concentration of 3 to 8 μg/ml in hybridization solution, and the sections were incubated overnight. Washes after hybridization were carried out in 1× SSC, 50 to 55% formamide, and 0.1% Tween 20. The entire process was performed at 65° to 72.5°C (the higher stringency was used for the PDGF-B probe). Production of digoxygenin (DIG)–labeled RNA probes and detection of the probes on sections with an alkaline phosphatase-conjugated antibody were accomplished with DIG-labeled uridine triphosphate, the DIG RNA Labeling Kit, and the DIG Nucleic Acid Detection Kit (Boehringer Mannheim) according to the manufacturer's instructions. PDGF-B sense and antisense probes were generated from a 0.8-kbp mouse cDNA containing the full-length coding sequence cloned in pBS-SK. PDGF-Rβ probes were generated from a 461-bp Sac I fragment cloned in pGEM-2. Figure 2 shows the use of antisense probes on 14-μm thick sections. Photography was done with a Nikon photomicroscope. Unstained sections and Normaski optics were used to allow for good sensitivity and resolution. Controls for the specificity of the in situ hybridization signals included sense probe hybridizations and PDGF-B antisense probe hybridization to PDGF-B −/− embryos. No hybridization signal was obtained in any of these controls (*14*). PDGF-Rβ expression was studied on 206 sections taken from seven littermate pairs of PDGF-B +/+ and −/− embryos. PDGF-B expression was studied on 108 sections taken from two PDGF-B +/+ and one PDGF-B −/− embryos. Representative examples of these analyses are shown in Figs. 2 and 3.
14. P. Lindahl, B. R. Johansson, P. Levéen, C. Betsholtz, data not shown.
15. M. C. Puri, J. Rossant, K. Alitalo, A. Bernstein, J. Partanen, *EMBO J.* **14**, 5884 (1995).
16. Because PDGF-B −/− mice show abrupt onset of hemorraging at late gestation, care was taken to select for analysis only nonhemorrhagic embryos, at the latest time point possible. Although *tie*^{lcz} up-regulation was invariably noticed in PDGF-B −/− brain capillaries, we also took care to apply PDGF-B +/+ and −/− tissue to the same histological glass slides to allow for parallel processing. The lacZ staining [B. Hogan, R. Beddington, F. Costantini, E. Lacy, *Manipulating the Mouse Embryo: A Laboratory Manual* (Cold Spring Harbor Laboratory Press, Cold Spring Harbor, NY, 1994)] was developed at different time points, and some sections were counter stained with erythrosin. Representative areas (Fig. 4) were selected from 296 sections analyzed in 15 embryos, five each of the genotypes PDGF-B +/+, *tie*^{lcz}/*tie*^{wt}; PDGF-B −/−, *tie*^{lcz}/*tie*^{wt}; and PDGF-B +/+, *tie*^{wt}/*tie*^{wt}.
17. P. Carmeliet *et al.*, *Nature* **383**, 73 (1996).
18. S. Davis *et al.*, *Cell* **87**, 1161 (1996).
19. C. Suri *et al.*, *ibid.*, p. 1171.
20. M. Vikkula *et al.*, *ibid.*, p. 1181.
21. J. Folkman and P. A. D'Amore, *ibid.*, p. 1153.
22. D. J. Dumont *et al.*, *Genes Dev.* **8**, 1897 (1994).
23. T. N. Sato *et al.*, *Nature* **376**, 70 (1995).
24. D. J. Dumont, T. P. Yamaguchi, R. A. Conlon, J. Rossant, M. L. Breitman, *Oncogene* **7**, 1471 (1992).
25. T. Kuwabara and D. G. Cogan, *Arch. Ophthalmol.* **69**, 492 (1963).
26. D. J. Crocker, T. M. Murad, J. C. Geer, *Exp. Mol. Pathol.* **13**, 51 (1970).
27. A. Orlidge and P. A. D'Amore, *J. Cell Biol.* **105**, 1455 (1987).
28. Y. Sato and D. B. Rifkin, *ibid.* **109**, 309 (1989).
29. J. Korhonen *et al.*, *Blood* **5**, 1828 (1995).
30. D. G. Cogan, D. Toussaint, T. Kuwabara, *Arch. Opthalmol.* **66**, 366 (1961).
31. S. M. Buzney, R. N. Frank, S. D. Varma, T. Tanishima, K. H. Gabbay, *Invest. Ophthalmol. Visual Sci.* **16**, 392 (1977).
32. P. Lindahl, L. Karlsson, P. Levéen, M. Pekny, M. Pekna, C. Betsholtz, in preparation.
33. R. Osterby, *Acta Med. Scand.* **574**, 1 (1974).
34. H. Boström *et al.*, *Cell* **85**, 863 (1996); D. Henrique *et al.*, *Nature* **375**, 787 (1995).
35. E. Shinbrot, K. G. Peters, L. T. Williams, *Dev. Dyn.* **199**, 169 (1994); L. Holmgren, A. Glaser, S. Pfeifer-Ohlsson, R. Ohlsson, *Development* **113**, 749 (1991).

36. We acknowledge G. Bokhede, S. Beckman, A. Casselbrant, Y Josefsson, L. Karlsson, and S. Tuneberg for technical help; A. Bernstein and M. Puri for supplying *tie*^{lcz} mice; M. Mercola, J. Escobedo, P. Soriano, and W. D. Richardson for probes; and the Swedish Cancer Foundation, the Swedish Medical Research Council (MFR), the IngaBritt and Arne Lundberg Foundation, and the Göteborg University for financial support.

15 January 1997; accepted 19 May 1997